Article

Not peer-reviewed version

Polyvinyl Alcohol Coatings Containing Lamellar Solids with Antimicrobial Activity

Maria Bastianini * , Michele Sisani , Raul Escudero Garcia , Irene Di Guida , Carla Russo , Donatella Pietrella , Riccardo Narducci *

Posted Date: 21 May 2024

doi: 10.20944/preprints202405.1396.v1

Keywords: LDH; LSH; cinnamate anions; salicylate anions; antimicrobial activity; PVA; PET

Article

Polyvinyl Alcohol Coatings Containing Lamellar Solids with Antimicrobial Activity

Maria Bastianini [1]*, Michele Sisani [1], Raúl Escudero García [1,2], Irene Di Guida [1], Carla Russo [3], Donatella Pietrella [3] and Riccardo Narducci [2]*

[1] Prolabin & Tefarm s.r.l., Via dell'Acciaio 9, 06134 Perugia, Italy.
[2] Dep. Industrial Engineering and International Laboratory "Ionomer Materials for Energy", Tor Vergata University of Rome, via del Politecnico 1, 00133 Roma, Italy.
[3] Dipartimento di Medicina e Chirurgia, Università degli Studi di Perugia, Piazzale Sereni, 1/8, 06129 Perugia, Italy
* Correspondence: maria.bastianinirolabintefarm.com, riccardo.narducci@uniroma2.it

Abstract: The design of an antimicrobial coating materials becomes ideal in order to prevent infections caused by the transmision of pathogens coming from human's contact with contaminated surfaces. In that aim layered single hydroxides (LSH) and layered double hydroxides (LDH) containing Zn and Cu, in nitrate form and intercalated with antimicrobial molecules, were synthesized and characterized. Cinnamate and salicylate anions were chosen to be intercalated in the fillers because of their well known antimicrobial activity. Several coatings based on polyvinyl alcohol (PVA) and LDH or LSH with increasing amounts of filler were prepared and filmed on a polyethylene terephthalate (PET) substrate. Coatings were characterized and their antimicrobial activity was evaluated against pathogens critical in nosocomial infections, giving interesting results.

Keywords : LDH; LSH; cinnamate anions; salicylate anions; antimicrobial activity; PVA; PET

1. Introduction

Over the 21st century, emerging infectious diseases (EIDs) have increased their incidence in the population and it seem to be an upwards tendency in the future. EIDs refer to emerging or drug-resistant infectious diseases that affect the human population. These diseases have their origin in the spread of many microorganisms, viruses, and other pathogens whose growth and inhibition becomes a challenge [1].

World Health Organization (WHO) classified antimicrobial resistance (AMR) as one of the most critical medical issues to be resolved. Bacteria responsible for AMR have been defined by the Infectious Disease Society of America and classified as ESKAPE pathogens: *Acinetobacter baumannii, Staphylococcus aureus, Klebsiella pneumoniae, Enterococcus faecium, Pseudomonas aeruginosa*, and *Enterobacter spp* [2]. ESKAPE pathogens belong both to gram-positive and gram-negative bacteria, and they are often responsible for serious nosocomial infections [3].

Reducing the spreading of the infection could be a help in fighting bacterial resistance against antibiotics. Coating surfaces that are directly in contact with human's daily life with antimicrobial and/or antiviral substances can be considered one of the most promising solutions. The global antimicrobial coatings market size was valued at USD 8.34 billion in 2020 and is expected to grow at a CAGR of 13%, reaching USD 20.71 billion by 2028 [4]. Nanoparticles of Cu and Zn are already used in contact killing surfaces with great efficacy. The antibacterial effect of Cu and Zn surfaces is attributed to a combination of the damage inferred by Cu(II) and Zn(II) ions released from the surface. They interact with reactive oxygen species (ROS), leading to lipid peroxidation and subsequent loss of membrane integrity, protein damage, DNA damage and cells death.

The aim of this work is to synthesize and characterize layered single (LSH) or double hydroxides (LDH) containing Cu and/or Zn, and use them to convey antimicrobial molecules in the interlayer region. Lamellar solids have been widely used in literature as carrier of antimicrobial molecules in different application, reaching interesting goals [5–7]. In that case, the idea is to combine the proven efficacy of the metals in the layer with that of conveyed molecules, reaching a synergistic effect. In detail ZnOH-LSH, ZnAl-LDH and ZnCuAl-LDH in nitrate from were synthesized as starting materials.

Cinnamate [8] (CA) and salicylate [9] (SAL) are two molecules both well known for their antimicrobial efficacy. They were selected because of their acidic nature, that gives them the ability to be easily intercalated as anions in both LSH and LDH.

Both molecules were conveyed in all solids, obtaining 6 materials: ZnOH-CA, ZnAl-CA, ZnCuAl-CA, ZnOH-SAL, ZnAl-SAL, and ZnCuAl-SAL. The pristine solids and the intercalated ones have been used as functionalizing filler in the preparation of coating resins based on PVA. Water based PVA resin is considered as an ecofriendly synthetic petroleum-based resins. It is an ideal resin for a coating because it is biocompatible, transparent, chemo-resistant, tough, a good barrier agent and can be industrially produced by non-petroleum routes implying low price production [10]. In literature PVA has already been functionalized with inorganic filler obtaining interesting perfomances [11,12]. Moreover, it has been also already functionalized with a ZnOH-SAL, demonstrating a good compatibility between the polymer and the filler [13]. However, the antimicrobial functionality was not explored.

LDH/PVA resin and LSH/PVA resin composites were successfully prepared and filmed on a PET substrate. Percentages of 1%, 5% and 10% of LSH and LDH were used. The films were characterized by X-Rays Diffraction spectroscopy (XRD), Fourier-transform infrared spectroscopy (FT-IR) and for their antimicrobial property.

2. Materials and Methods

2.1. Materials

Zinc nitrate hexahydrate [$Zn(NO_3)_2 \times 6H_2O$], copper nitrate hexahydrate [$Cu(NO_3)_2 \times 6H_2O$], aluminium nitrate nonahydrate [$Al(NO_3)_3 \times 9H_2O$], trans-cinnamic acid (97%), were purchased from Sigma-Aldrich. Sodium salicylate (99.83%) was purchased from Polichimica S.R.L (Bologna, Italia). Urea, sodium hydroxide (NaOH) was purchased from Sigma-Aldrich. Polyvinyl alcohol resin (Sealcoat HS 25) was purchased from Baumeister.

2.2. Synthesis of ZnOH-LSH, ZnAl-LDH, ZnCuAl-LDH in Nitrate Form

The synthesis of ZnOH-LSH in nitrate form was conducted according to Li et al. [14] method. The molar ratio of OH/Zn used was 1.6. 80 mL of a 0.2 M NaOH solution was dropped into a 50 mL solution containing 10 mmol of $Zn(NO_3)_2 \times 6H_2O$, under mechanical stirring at room temperature. A white precipitate was obtained. The syntheses of ZnAl-NO_3 and ZnCuAl-NO_3 were conducted following the urea hydrolysis method [15,16]. For ZnAl-NO_3 an aqueous solution containing Al^{3+} and Zn^{2+} with the molar fraction $Al^{3+}/(Al^{3+} + Zn^{2+})$ equal to 0.33 was prepared by dissolving $Al(NO_3)_3 \times 9H_2O$ and $Zn(NO_3)_2 \times 6H_2O$ in distilled water at 1 M concentration. To this solution solid urea was added until the molar ratio of urea/Al3+ reached 4.0. The clear solution was refluxed for 24 h, and a white precipitate was obtained. For ZnCuAl-NO_3 an aqueous solution containing Al^{3+},Zn^{2+},Cu^{2+} with the molar fraction $Al^{3+}/(Al^{3+} + Zn^{2+} + Cu^{2+})$ equal to 0.33 and a ratio Zn^{2+}/Cu^{2+} equal to 2.5, was prepared by dissolving $Al(NO_3)_3 \times 9H_2O$, $Zn(NO_3)_2 \times 6H_2O$ and $Cu(NO_3)_2 \times 6H_2O$ in distilled water at 1 M concentration. To this solution solid urea was added until the molar ratio of urea/Al^{3+} reached 4.0. The obtained solution was poured into a reactor under mechanical stirring, fixing the temperature of reaction at 90 °C for 24 h. A light blue precipitate was obtained. After the syntheses all the precipitates were centrifuged, washed twice to remove excess of urea and ions, dried in oven at 60 °C until constant weight and grounded using a knife mill. The obtained solids were sieved with an 80 micron mesh sieve.

doi:10.20944/preprints202405.1396.v1

2.3. Intercalation of Cinnamate and Salicylate in ZnOH-LSH, ZnAl-LDH and ZnCuAl-LDH

The intercalation of cinnamic acid was carried out as following. Cinnamic acid was salified by addiction of a stoichiometric amount of NaOH 1 M solution. The as-obtained salt was dissolved in a mixture ethanol/water 1:1 in order to obtain a concentration of 0.1 M. ZnOH-LSH, ZnAl-LDH and ZnCuAl-LDH were equilibrated with the cinnamate solution under mechanical stirring for 24 h, in order to obtain the following intercalation product: ZnOH-cinnamate (ZnOH-CA), ZnAl-cinnamate (ZnAl-CA), ZnCuAl-cinnamate (ZnCuAl-CA). Mass/volume ratios used were 1 g/54 mL for ZnOH-LSH, 1 g/56 mL for ZnAl-LDH and ZnCuAl-LDH respectively. For the preparation of the second intercalation product a water solution of sodium salicylate 0.5 M was prepared. The solids in nitrate form were equilibrated with the salicylate solution under mechanical stirring for 24 h, in order to obtain the respective intercalation compound: ZnOH-salicylate (ZnOH-SAL), ZnAl-salicylate (ZnAl-SAL), ZnCuAl-salicylate (ZnCuAl-SAL). Solid/volume ratios used were: 1 g/10.4 mL for ZnOH-LSH, 1 g/11.2 mL for ZnAl-LDH and ZnCuAl-LDH respectively. Intercalations were carried out at room temperature, the resulting compounds were recovered by centrifugation, washed twice with deionized water, dried in oven at 60 °C and grounded using a knife mill. The obtained solids were sieved with an 80 micron mesh sieve.

2.4. Coating Resin Composite of PVA/LDH and PVA/LSH Preparation

Composite coatings were prepared mixing PVA resin dissolved in water with a weighted amount of LDH and LSH powders. The exact amount of PVA, water and filler for the indicated percentage are reported in Table I. The dispersions were prepared using as filler: ZnOH-LSH, ZnAl-LDH and ZnCuAl-LDH, ZnOH-CA, ZnAl-CA, ZnCuAl-CA, ZnOH-SAL, ZnAl-SAL, and ZnCuAl-SAL at the following weight percentage: 1, 5, 10 %. The films were labelled using the filler name and the relative percentage used, i.e. ZnAl-LDH 1%, etc. A PVA film reference was also prepared. After mixing using magnetic stirring, ultrasound was applied in order to assure a homogenous dispersion of the lamellar solid into the matrix. Few drops of 1M NaOH solution were poured in order to catalyze the polymerization.

Table I. amount of PVA, water and filler used for the preparation of the dispersion used for the coatings**.**

Film	PVA amount (g)	Water (mL)	Filler (g)
1%	9.9	100	0.1
5%	9.5	100	0.5
10%	9.0	100	1.0

2.5. Deposition of Resin Composite on PET Substrate

PET samples, with dimensions of 7.5x3.6 cm were coated with the as-prepared resins. 5 mL of the dispersion were poured on the substrate. The resin was filmed by manually rolling the product with a mayer's bar number 25. 2 layers of the resins containing fillers were deposed on each substrate. After the adhesion of both layers, each sample was dried in an oven at 60 °C for 7-10 minutes. The films obtained were characterized by XRD and FT-IR spectroscopies.

2.6. Microorganisms

The antimicrobial tests were carried out on the following pathogens: two *gram-positive* bacteria *Staphylococcus aureus* (ATCC 29213) and the clinical isolate *Enterococcus faecalis*, two gram-negative clinical isolates bacteria *Acinetobacter baumannii, Klebsiella pneumoniae* and the yeast *Candida albicans* (SC5314). Bacteria were grown in Muller Hinton agar (MHA), whereas Candida cells in Sabouraud agar. One colony of each microorganism was inoculated in the appropriate culture broth medium (Muller Hinton broth MHB or Sabouraud broth) and maintained for 24 h at 37 °C. Then, after centrifugation, the recovered microorganisms were washed twice in sterile saline and counted by

doi:10.20944/preprints202405.1396.v1

spectrophotometric analysis. The suspensions were then diluted in sterile saline to the concentration required in the following assays.

2.7. Antimicrobial Susceptibility Test

Antimicrobial susceptibility test was performed using the Kirby–Bauer disk diffusion method following the guidelines of the clinical and laboratory standard institute (CLSI) [17]. Bacterial sensitivity was tested for the films, erythromycin and fluconazole were used as positive control inhibiting bacteria strains and yeast, respectively. Films were cut in 5 mm diameter disks and sterilized under UV rays for 60 minutes. Muller Hinton agar plates were used for testing different bacteria. After adjusting the bacterial suspension to the concentration of 0.5 McFarland in sterile saline, the suspension was spread on the agar plate by streaking a swab three times over the entire agar surface rotating the plate approximately 60 degrees each time to ensure a homogeneous distribution of the inoculum. Films were placed on the top of the culture plates and incubated for 24 h at 37 °C. Using a ruler each inhibition zone were measured. Results are expressed as zone of inhibition (ZOI) measured in mm. Data are the mean ±SD of three different experiments.

2.8. Analytical Procedures and Instrumentation

2.8.1. Inductively Coupled Plasma-Optical Emission Spectrometer

The solids were dissolved in water using a proper amount of HNO3, in order to determine Zn, Al and Cu content. The solutions were analyzed after a proper dilution by ICP-OES Perkin Elmer, Avio 200.

2.8.2. X-Rays Diffraction Spectroscopy

X-ray powder diffraction (XRD) patterns were recorded with a Bruker D2 Phaser diffractometer operating at 30 kV and 15 mA, step size of 0.02 2θ degrees and time per step of 1 s, using the Cu Kα radiation (1.54 Å) and multistrip LYNXEYE SSD160 detector.

2.8.3. FT-IR Analysis

FT-IR spectra were recorded at room temperature using a FT-IR-ATR Nicolet 380 (Thermo Fisher, Waltham, MA, USA). Typically, each spectrum was obtained in the spectral region from 400 to 4000 cm^{-1}. For the data collection17, an attenuated total reflection crystal in SeZn was used.

2.8.4. Thermal Analysis

Thermogravimetric analysis (TGA) of the samples were carried out with a Perkin Elmer STA 8000, in air flow with at heating rate of 10 °C min^{-1}.

2.8.5. UV-Vis Analysis

UV-visible analyses were carried out by UV-visible double-beam spectrophotometer (Jasco V-750, Oklahoma City, OK, USA). The salicylate and cinnamate content in the samples was determined by UV-Vis spectroscopy. A weighed amount of the sample (~20 mg) was completely dissolved in 100 mL of a 0.85 M aqueous solution of HCl. Salicylate and cinnamate in the samples were determined by monitoring the maximum absorption value of the molecules after calibration and proper dilution. A suitable calibration was carried out by dissolving known amounts of pure salicylate or cinnamate in a proper volume of a 0.85 M aqueous solution of HCl. Five standards and a blank sample were then prepared and analyzed in order to obtain the calibration curve.

3. Results and Discussion

3.1. Characterization of the Pristine Powders

The aim of this work is to synthesize and characterize lamellar solids for the vehiculation of antimicrobial molecules and test their antimicrobial activity. In literature this intercalation compounds have widely demonstrated to possess interesting properties [6,7,18] in this field, for application in the preparation of active polymer composites in wound healing and food packaging. We explore for the first time the application of this intercalation compounds for the preparation of antimicrobial coatings. ZnOH-LSH, ZnAl-LDH and ZnCuAl-LDH were chosen as filler, due to the presence of Zn and Cu that have a well documented antimicrobial activity [4] The powders have been prepared as described in the experimental part and characterized by XRD and ICP-OES. XRD spectra are reported in Figure 1.

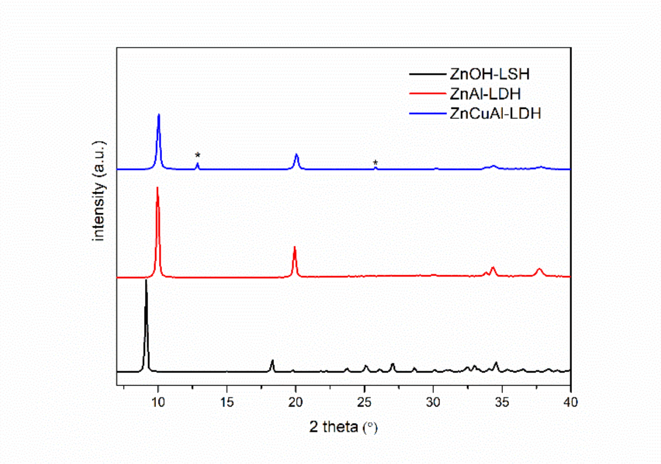

Figure 1. ZnOH-LSH black line, ZnAl-LDH red line, and ZnCuAl-LDH blue line.

The first reflex of ZnOH-LSH is at 2θ=9.2 that corresponds to the (200) diffraction peak and to an interlayer distance of 9.6 Å. These values are compatible with the presence of nitrate in the interlayer region [14] For ZnAl-LDH and ZnCuAl-LDH the strongest peak at 2θ = 9.9, due to (003) reflection [19], can be related to an interlayer distance of 8.9 Å, corresponding in both case to the gallery height tributable to nitrate [15]. In case of ZnCuAl-LDH a very small amount of a second phase (underlined with *) is present, probably tributable to garhardtite [20], chemical formula $Cu_2(NO_3)(OH)_3$. ICP-OES results allowed to calculate the following chemical formulae: $Zn_5(OH)_8(NO_3)_2$ x $2H_2O$, $Zn_{0.70}Al_{0.30}(OH)_2(NO_3)_{0.30}$ x 0.5 H_2O and $Zn_{0.55}Cu_{0.05}Al_{0.40}(OH)_2(NO_3)_{0.40}$ x 0.5 H_2O. An interesting observation is that the interlayer space of ZnOH-NO_3 has the biggest value, that can be probably associated to the higher number of water molecules coordinated directly to the structure [21]. FTIR spectra on the obtained powders are reported in Figure 1 of the SI. The ZnOH-NO_3 spectrum (black line) is similar to the one reported by *Ruiz et al.* [22]. The bands at 3573 cm^{-1} and 3462 cm^{-1} correspond to O-H stretching vibrations of the lattice and of water molecules occupying the interlayer region respectively. The sharp band at 1636 cm^{-1} can be assigned to the bending mode of intercalated water molecules. The broad band located at 1367 cm^{-1} is due to the asymmetric stretching vibration of nitrate groups. The ZnAl-NO_3 spectrum (red line) presents a signal at 3378 cm^{-1} indicating the presence of water molecules [23]. The band broadening is due to H-bond stretching vibrations of OH groups in the brucite-like layers and in intercalated water molecules. The presence of water in the interlayer region is confirmed by the signal at 1636 cm^{-1} associated to the bending mode of water molecules occupying the interlamellar region [24]. A sharp band at 1341 cm^{-1} is characteristic of the asymmetric stretch vibration of nitrate groups. Regarding to ZnCuAl-NO_3 spectrum (blue line), the nitrate band is observed at 1346 cm^{-1} while the vibration at 1415 cm^{-1} probably corresponds to a symmetry reduction of the carbonate anions. As reported by *Palacio et al.* [25] a broad peak appears at around 3481 cm^{-1}, always associated to H-bond stretching mode of vibrations from OH groups in the structure and from water molecules between the layers and physisorbed. The band at 1636 cm^{-1} is due to the intercalated water bending.

3.2. Characterization of the Intercalated Powders

The XRD spectra of the three cinnamate intercalation compounds are reported in Figure 2.

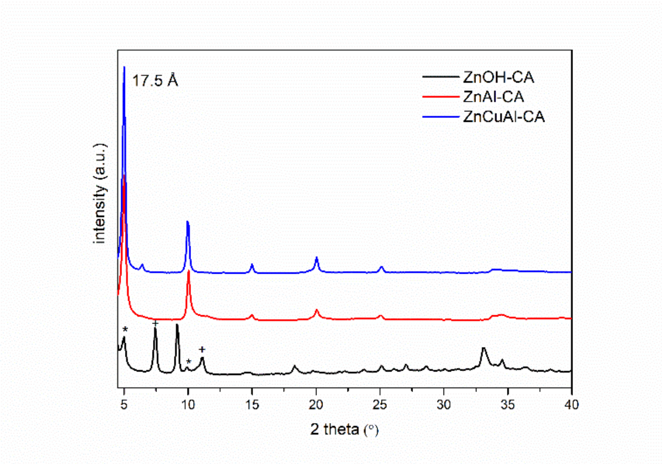

Figure 2. ZnOH-CA black line, ZnAl-CA red line, and ZnCuAl-CA blue line.

In each case it is possible to observe an increase of interlayer distance from the starting nitrate forms (8.9 Å for LDH and 9.6 Å for LSH) up to 17.5 Å, due to the effective intercalation of the organic anions. ZnOH-CA spectra (black line) shows a mixture of three different phases. The peaks at 11.8 Å and 7.9 Å (indicated with +) are probably the second and third reflexes (004 and 006 respectively) of the intercalation compound with an interlayer distance of 23.6 Å. This can be attributed to an intercalated phase of cinnamate, in which the LSH possesses a type IIb structure [26]. This is formed by one quarter of the octahedral zinc cations displaced from main layer to tetrahedral sites located above and below each empty tetrahedron [27]. A second phase (indicated with *) has a first reflex corresponding to an interlayer distance of 17.5 Å as observed for ZnAl-CA and ZnCuAl LDHs. It is likely this phase derives from the type I structures, were metal centers are only coordinated in an octahedral arrangement like in layered double hydroxide [27]. A partial residue of nitrate phase was also observed at 9.6 Å. ZnAl-CA and ZnCuAl-LDH phases present both an interlayer distance of 17.5 Å, compatible with cinnamate intercalation [23], and no residual nitrate was detected in both cases. According to *Adam et al's.* [23] model, the anions were considered in this phase to be orientated in bilayer, where the molecules are partially tilted respect to the plane. FTIR spectra on the cinnamate intercalated powders are reported in Figure 2 of the SI and they cleary confirm the XRD data, indicating the presence of cinnamate in the powders. The compounds exhibit most of the vibrations assigned to cinnamate, even if some vibrations are slightly shifted due to the electrostatic interaction between the organic anion and the inorganic layered structure [23,26]. First, vibrations due to trans-C-H out-of-plane bending (974 cm^{-1}) are clearly evident in all the three samples. Moreover, COO^{-} stretching of intercalated cinnamate anion appeared at 1531 and 1390 cm^{-1}. Also C=C stretching signal is present in all the samples at 1636 cm^{-1}. In the ZnOH-CA spectrum the band at 1370 cm^{-1} confirms the presence of a certain amount of residual nitrate, as observed in the XRD spectrum.

XRD spectra of the three compounds recovered after the contact with salicylate solutions are reported in Figure 3. In this case the intercalation of salicylate was successful only with ZnAl-LDH, obtaining a pure phase. The increase of interlayer distance from 8.9 Å to 16.5 Å confirms the presence of salicylate between the lamellae [6].

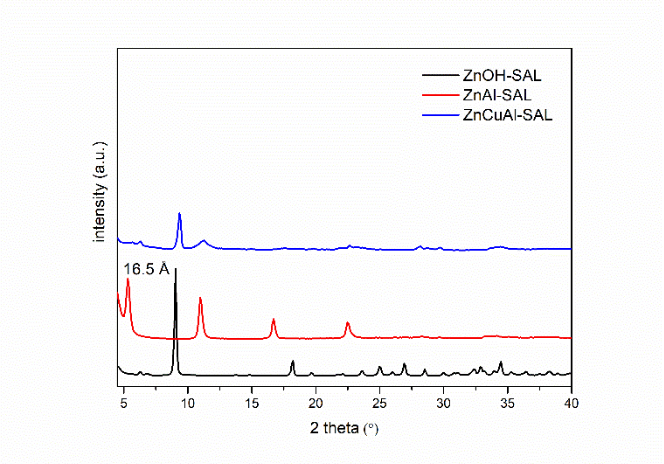

Figure 3. ZnOH-SAL black line, ZnAl-SAL red line, and ZnCuAl-SAL blue line.

Both ZnOH-SAL and ZnCuAl-SAL are still in the pristine nitrate form, with an evident increasing of the turbostratic disorder, especially for the ZnCuAl-SAL sample. In this last sample we also observed a change of color, from light blue to light green. This change is probably due to a complex formation. The loss of an effective intercalation can be attributed to many factors, but a detailed discussion falls outsite the scope of this paper. Moreover, salicylate is detected in all the three compound as demonstrated by the FT-IR (Figure 3 of SI). Regarding ZnAl-SAL spectrum, a clear evidence of SAL presence are the asymmetric and symmetric stretching modes of the COO$^-$ group observed at 1565 and 1360 cm^{-1}. These bands occur at slightly lower wave-numbers in comparison to the free COO$^-$ functional group in salicylate, according to literature [27]. Also, the peak at 1252 cm^{-1} is due to the OH bending vibration mode of the phenolic group [13]. In the ZnOH-SAL spectrum the bands due to the pristine solid are still present but the typical signals of salicylate can be also detected. At 1570 cm^{-1} is evident the asymmetric stretching mode of salicylate, while the symmetric one is probably covered by the nitrate signal. The band at 1250 cm^{-1} due to the OH bending vibration mode of the phenolic group is also present. ZnCuAl-SAL spectrum shows signals different from those observed for ZnAl-SAL. *Salavati-Niasari et al.* [28] reported a FTIR spectrum of [Cu(Hsal)$_2$] with very similar band positions, giving an evidence of a partial formation of a copper-salicylate complex. The presence of bands at 1564 and 1605 cm^{-1} is due to metal-bonded C–O and the bands at 1407 and 1335 cm^{-1} are due to the C–C bond of the salicylate group. This result indicates that in ZnOH-SAL the organic molecules are probably adsorbed on the surface of the solid; while in ZnCuAl-SAL a certain amount of [Cu(Hsal)$_2$] has been formed. It can be concluded that even if the intercalation was not achieved, nevertheless the samples are both interesting candidates for testing the antimicrobial properties, since they clearly contain a suitable amount of antimicrobial species. All the samples were characterized by TGA in order to calculate the amount of conveyed molecules. The UV-vis analysis carried out on the dissolved samples confirmed the observed results. In Table II are summarized the obtained results and the calculated amount of organic molecule in each compound. In the sample ZnOH-SAL the organic molecule is probably absorbed on the surface.

Table II. water loss and total loss observed in the TGA of each sample, active content in weight % in the obtained compounds calculated by TGA and confirmed by UV-Vis.

Sample	Water loss %	Total Loss %	Active weight content %
ZnOH-CA	4,0	49,5	37
ZnAl-CA	18,0	54,4	27
ZnCuAl-CA	12,0	51,0	30
ZnOH-SAL	5,0	53,0	35
ZnAl-SAL	21,0	56,8	25
ZnCuAl-SAL	5,0	53,1	30

3.3. Chemical-Physical Characterization of the Coatings

Coatings were prepared by mixing PVA resin with a weighted amount of the prepared filler. Then the as-prepared resins were coated on PET samples (7.5x3.6 cm). 5 mL of the resin dispersion were poured on the substrate and filmed by rolling the product with a Mayer's bar as described previously (Figure 4). 2 layers of the resins containing fillers were deposed on each substrate.

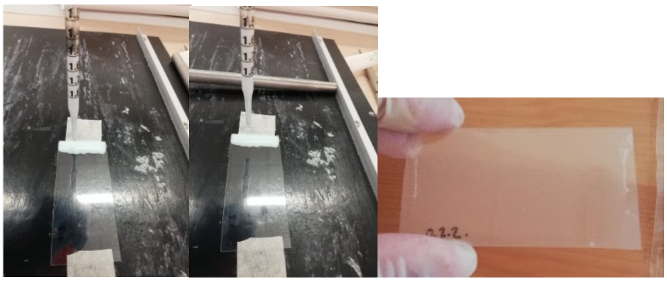

Figure 4. Image showing the step of pouring a layer of resin onto PET sheet (**left**), showing the Mayer's bar spreading the resin along the whole sheet (middle) and showing the final product after been dried in the oven (**right**).

All the obtained films were characterized by XRD and FT-IR, but for sake of simplicity here are reported only the characterization on the following film: ZnOH-LSH 1%, ZnOH-LSH 5% ZnOH-LSH 10%. Same considerations can be obtained analysing the XRD data of the other composite films.

In Figure 5 XRD spectra are reported. It is worth to notice that no change of the interlayer distance is detected and the first reflex of the intercalate is always visible, meaning that no significant interaction are observed between the filler and the polymer (i.e. formation of intercalated composited or nanometric dispersion of the filler). The intensity of the first reflex increase linearly with the increase of filler content.

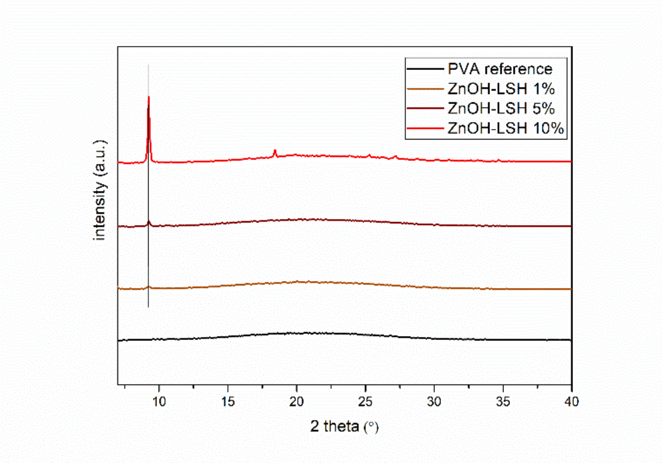

Figure 5. PVA black line, ZnOH-LSH 1% brown line, ZnOH-LSH 5% dark red line, ZnOH-LSH 10% red line**.**

FTIR analysis on the ZnOH-LSH films, compared with the spectra of the substrate and of the pure powder are reported in Figure S4. All the spectra present the same bands at similar positions due to the PVA-PET support and the most intense signal of ZnOH-LSH 1370 cm^{-1}. The spectrum of PVA-PET film exhibited bands in the range of 1412–1325 cm^{-1}, ascribed to the bending of CH_2 groups. A characteristic signal of stretching vibration band of C=O is visible at 1733 cm$^{-1.}$ C-O-C stretching vibration band are detectable at 1091 cm^{-1} and 1244 cm^{-1}, suggesting the presence of an ester linkage between hydroxyl group of PVA and carboxyl groups of PET.

3.4. Antimicrobial Tests on the Coatings

The antimicrobial assays were carried out on ATCC strains and clinical isolates *S. aureus, E. faecalis, A. baumannii, K. pneumoniae* and *C. albicans.* Among them, it is important to underline that *S. aureus, A. baumannii, K. pneumoniae* are considered as ESKAPE pathogens [3], so find new strategies to reduce their spreading is a really critical issue. The antibacterial properties of films were determined using the disk-diffusion Kirby–Bauer test according to directions of Clinical Laboratory Standards Institute [17]. Erythromycin and fluconazole were used as positive control. Coatings containing ZnAl-LDH, ZnCuAl-LDH, ZnOH-LSH were active against *S. aureus*, *E. faecalis* and *C. albicans*, as reported in Table III. In ZnAl-LDH and ZnOH-LSH the antimicrobial performance increased with the increase of Zn content. That is in concordance with the study of *Cheng et al.* [30] that concludes that LDH, and LSH as well [22], are a reservoir of zinc ions, and can slowly release that metals reaching an effective antimicrobial activity.

Table 3. zone of inhibition (ZOI) measured in mm as mean ±SD of three different experiments of the coatings containing ZnAl-LDH, ZnCuAl-LDH, ZnOH-LSH. Results are expressed as zone of inhibition (ZOI) measured in mm. Data are the mean ±SD of three different experiments. NA: No Activity; NT: Not Tested.

	S. aureus	*E. faecalis*	*A. baumannii*	*K. pneumoniae*	*C. albicans*
ZnAl-LDH 1%	6.33±1.53	8.00±3.61	NA	NT	7.00±0.00
ZnAl-LDH 5%	7.33±2.08	7.33±2.52	NA	NT	7.00±0.00
ZnAl-LDH 10%	7.33±2.08	8.67±3.21	NA	NT	8.33±1.53
ZnCuAl-LDH 1%	NA	NA	NA	NA	6.33±0.58
ZnCuAl-LDH 5%	NA	5.08±3.04	NA	NA	6.33±1.15
ZnCuAl-LDH 10%	NA	NA	NA	NA	8.00±1.00
ZnOH-LSH 1%	NA	8.33±1.53	NA	NT	7.67±3.79
ZnOH-LSH 5%	NA	10.33±0.58	NA	NT	9.33±4.93
ZnOH-LSH 10%	8.33±3.06	11.3±2.08	7.33±2.08	NT	11.00±3.61
Erythromycin	16.33±1.15	20.00±2.65	14.00±2.65	NA	
Fluconazole					5.67±1.15

Coatings functionalized with ZnAl-CA, ZnCuAl-CA, ZnOH-CA are active against *E. faecalis* and *C. albicans* (Table III). It is worth to underline that ZnCuAl-CA is active also against *K. pneumoniae* [31], that is now considered one of the most dangerous for public health because its antimicrobial resistance, especially for the high mortality rate. This behavior is probably due to the combined release of Zn^{2+}, Cu^{2+}, and cinnamate.

Table III. Zone of inhibition (ZOI) measured in mm as mean ±SD of three different experiments of the coatings containing ZnAl-CA, ZnCuAl-CA, ZnOH-CA. Results are expressed as zone of inhibition (ZOI) measured in mm. Data are the mean ±SD of three different experiments. NA: No Activity; NT: Not Tested**.**

	S. aureus	*E. faecalis*	*A. baumannii*	*K. pneumoniae*	*C. albicans*
ZnAl-CA 1%	NA	7.00±0.00	NA	NT	5.33±0.58
ZnAl-CA 5%	NA	8.00±4.41	NA	NT	8.67±3.79
ZnAl-CA 10%	NA	10.00±1.73	NA	NT	12.33±0.58
ZnCuAl-CA 1%	NA	NA	NA	5.33±0.58	5.33±0.58
ZnCuAl-CA 5%	NA	5.67±4.17	NA	5.33±0.58	7.00±1.00
ZnCuAl-CA 10%	NA	5.50±3.73	NA	6.00±1.00	11.33±1.15
ZnOH-CA 1%	NA	10.00±5.00	NA	NT	NA
ZnOH-CA 5%	NA	10.67±6.22	NA	NT	5.67±1.15
ZnOH-CA 10%	NA	10.00±6.22	NA	NT	8.00±1.00
Erythromycin	16.33±1.15	20.00±2.65	14.00±2.65	NA	
Fluconazole					5.67±1.15

Table IV. Zone of inhibition (ZOI) measured in mm as mean ±SD of three different experiments of the coatings containing ZnAl-SAL, ZnCuAl-SAL, ZnOH-SAL. Results are expressed as zone of inhibition (ZOI) measured in mm. Data are the mean ±SD of three different experiments. NA: No Activity; NT: Not Tested.

	S. aureus	*E. faecalis*	*A. baumannii*	*K. pneumoniae*	*C. albicans*
ZnAl-SAL 1%	6.33±1.15	9.67±5.03	NA	NT	6.67±2.89
ZnAl-SAL 5%	7.00±2.00	10.00±4.36	7.00±2.00	NT	7.33±4.04
ZnAl-SAL 10%	8.00±2.65	12.33±2.31	5.67±1.15	NT	7.00±3.46
ZnCuAl-SAL 1%	NA	5.42±3.30	7.33±4.04	10.00±5.20	NA
ZnCuAl-SAL 5%	8.33±1.53	6.57±3.49	9.00±6.93	10.00±2.65	6.50±2.12
ZnCuAl-SAL 10%	9.33±1.53	6.49±3.46	10.67±7.37	11.33±2.31	NA
ZnOH-SAL 1%	NA	7.33±2.52	9.67±3.79	NT	5.33±0.58
ZnOH-SAL 5%	NA	6.67±2.89	10.00±4.36	NT	6.00±1.73
ZnOH-SAL 10%	NA	9.00±5.29	10.33±4.16	NT	10.33±4.16
Erythromycin	16.33±1.15	20.00±2.65	14.00±2.65	NA	
Fluconazole					5.67±1.15

In Table IV are reported the results about coatings functionalized with ZnAl-SAL, ZnCuAl-SAL, ZnOH-SAL. Samples containing salycilate are the most interesting, confirming a synergistic activity of this antimicrobial molecule with $Zn^{2+}$and Cu^{2+}. They are all active against *S. aureus, E. faecalis, A. baumannii, K. pneumoniae* and *C. albicans.* The ZnCuAl-SAL ones are also active against *K. pneumoniae.* The wide activity of this sample can be also tribute to the partial formation of $[Cu(Hsal)_2]$, that possess an already documented antimicrobial activity [32].

5. Conclusions

In this work innovative surface coating materials to prevent pathogen infections by simple contact were designed. Polyvinyl alcohol resin solution with an increasing amounts of active fillers made up of intercalated cinnamate and salicylate in LDH or LSH were prepared and coated on a PET substrate. The materials were characterized with different techniques ICP-OES, XRD, FT-IR and TGA. The antimicrobial susceptibility test was performed using the Kirby–Bauer disk diffusion method. Coatings containing ZnAl-LDH, ZnCuAl-LDH, ZnOH-LSH were active against bacteria and yeast, the antimicrobial performance increased with the increase of Zn content. Samples containing salicylate presents a synergistic activity of this antimicrobial molecule with Zn^{2+} and Cu^{2+} ions. The ZnCuAl-CA and ZnCuAl-SAL are also active against the dangerous *K. pneumoniae*. Although this study is preliminary and requires further future investigation, nevertheless the results clearly indicate that the use of these coatings will certainly be useful for preventing the spread of microbes that cause even fatal diseases and with significant money savings for public health.

Supplementary Materials: The following supporting information can be downloaded at: www.mdpi.com/xxx/s1, Figure S1: FT-IR spectra of the powders, ZnOH-LSH black line, ZnAl-LDH red line, ZnCuAl-LDH blue line, Figure S2: FT-IR spectra of the powders, ZnOH-CA black line, ZnAl-CA red line, ZnCuAl-CA blue line, Figure S3: FT-IR spectra of the powders, ZnOH-SAL black line, ZnAl-SAL red line, ZnCuAl-SAL blue line, Figure S4: PVA black line, ZnOH-LSH 1% brown line, ZnOH-LSH 5% dark red line, ZnOH-LSH 10% red line, ZnOH-LSH

Maria Bastianini: Conceptualization, Methodology, Writing - Original draft preparation, Writing - Review & Editing, Visualization. **Michele Sisani:** Conceptualization, Methodology, Resources. **Raúl Escudero García:**

Investigation, Writing - Original draft preparation, Visualization. **Irene di Guida:** Validation, Investigation. Donatella Pietrella: Investigation, Writing - Original draft preparation. **Carla Russo:** Validation, Investigation. **Riccardo Narducci:** Conceptualization, Methodology, Writing - Original draft preparation, Writing - Review & Editing.

Funding: This research received no external funding.

Acknowledgements: Raúl Escudero García is grateful for the Erasmus Mundus Chemical Nanoengineering (CNE) master program and the scholarship support.

Conflicts of interest: The authors declare no conflict of interest.

References

1. Zhang, Y.; Fan, W.; Sun, Y. ; Chen, W. ; Zhang, Y.; Application of antiviral materials in textiles: A review. *Nanotechnol. Rev.* **2021**, *10*, 1092–1115. https://doi.org/10.1515/ntrev-2021-0072.
2. Mingoia, M. ; Conte, C. ; Rienzo, Di A. ; Dimmito, M.P. ; Marinucci, L. ; Magi, G. ; Turkez, H. ; Cufaro, M.C. ; Del Boccio, P.; Di Stefano, A.; Synthesis and Biological Evaluation of Novel Cinnamic Acid-Based Antimicrobials. *Pharmaceuticals* **2022**, *15*, 228. https://doi.org/10.3390/ph15020228.
3. Mulani, M. S. ; Kamble, E. E. ; Kumkar, S. N. ; Tawre, M. S; Pardesi, K. R. ; Emerging strategies to combat ESKAPE pathogens in the era of antimicrobial resistance: A review. *Front. Microbiol.* **2019**, *10*. https://doi.org/10.3389/fmicb.2019.00539.
4. Birkett, M.; Dover, L.; Cherian Lukose, C.; Wasy Zia, A.; Tambuwala, M.M.; Serrano-Aroca, Á.; Recent Advances in Metal-Based Antimicrobial Coatings for High-Touch Surfaces. *Int. J. Mol. Sci.* **2022**, *23*, 1162. https://doi.org/10.3390/ijms230311625.
5. Bastianini, M.; Scatto, M.; Sisani, M.; Scopece, P.; Patelli, A.; Petracci, A.; Innovative Composites Based on Organic Modified Zirconium Phosphate and PEOT/PBT Copolymer. *J.Compos.Sci.* **2018**, *2*, 31.https://doi.org/10.3390/jcs2020031.
6. Coiai, S.; Cicogna, F.; Pinna, S; Spiniello, R.; Onor, M.; Oberhauser, W.; Coltelli, M.-B.; Passaglia, E.; Antibacterial LDPE-based nanocomposites with salicylic and rosmarinic acid-modified layered double hydroxides, *Appl. Clay Sci.* **2021**, *214*, 106276. https://doi.org/10.1016/j.clay.2021.106276.
7. Puccetti, M. ; Donnadio, A.; Ricci, M.; Latterini, L.; Quaglia, G.; Pietrella, D.; Di Michele A.; Ambrogi, V.; Alginate Ag/AgCl Nanoparticles Composite Films for Wound Dressings with Antibiofilm and Antimicrobial Activities. *J. Funct. Biomater.* **2023**, *14*. https://doi.org/10.3390/jfb14020084.
8. Guzman, J. D.; Natural cinnamic acids, synthetic derivatives and hybrids with antimicrobial activity. *Molecules*, **2014**, *19*, doi: 10.3390/molecules191219292.
9. Sykes, E. M. E.; White, D.; McLaughlin, S.; Kumar, A.; Salicylic acids and pathogenic bacteria: New perspectives on an old compound. *Can. J. Microbiol.* **2023**, *14*, 1–14. doi: 10.1139/cjm-2023-0123. .
10. Moulay, S.; Review: Poly(vinyl alcohol) Functionalizations and Applications. *Polym. - Plast. Technol. Eng.* **2015**, *54*, 1289–1319. https://doi.org/10.1080/03602559.2015.1021487.
11. Yeun, J. H.; Bang, G. S.; Park, B. J.; Ham, S. K.; Chang, J. H. Poly(vinyl alcohol) nanocomposite films: Thermooptical properties, morphology, and gas permeability. *J. Appl. Polym. Sci.* **2006**, *101*, 591–596. https://doi.org/10.1002/app.23372.
12. Bastianini, M.; Sisani, M.; Naryyev, E.; Petracci, A.; Di Guida, I.; Narducci. R. Composite membranes based on polyvinyl alcohol and lamellar solids for water decontamination. *New J. Chem.*, **2024**, *48*, 2128. https://doi.org/10.1016/j.mtchem.2023.101381.
13. Ruiz, C. V.; López-González, M.; Giraldo, O.; Composite films based on salicylic acid-layered zinc hydroxide and polyvinyl alcohol: Preparation, characterization, properties and potential applications. *Polym. Test.* **2021**, *94*. https://doi.org/10.1016/j.polymertesting.2021.107057.
14. Li, P.; Xu, Z. P.; Hampton, M. A.; Vu, D. T.; Huang, L.; Rudolph, V.; Nguyen, A. V.; Control preparation of zinc hydroxide nitrate nanocrystals and examination of the chemical and structural stability. *J. Phys. Chem. C*, **2012**, *116*, 10325–10332. DOI: 10.1021/jp300045u.
15. Bastianini, M.; Vivani, R.; Nocchetti, M.; Costenaro, D.; Bisio, C.; Oswald, F.; Meyer, T.B.; Marchese, L. Effect of iodine intercalation in nanosized layered double hydroxides for the preparation of quasi-solid electrolyte in DSSC devices. *Sol. Energy* **2014**, *107*, 692–699. https://doi.org/10.1016/j.solener.2014.06.014.
16. Costantino, U.; Marmottini, F.; Sisani, M.; Montanari, T.; Ramis, G.; Busca, G.; Turco, M.; Bagnasco, G. Cu-Zn-Al hydrotalcites as precursors of catalysts for the production of hydrogen from methanol. *Solid State Ionics* **2005**, *176*, 2917–2922. https://doi.org/10.1016/j.ssi.2005.09.051.
17. Clinical and Laboratory Standards Institute (CLSI). Clinical and Laboratory Standards Institute Methods for Dilution Antimicrobial Susceptibility Tests for Bacteria That Grow Aerobically Standard, Approval CDM-A.; *M07 Methods dilution Antimicrob. Susceptibility Tests Bact. That Grow Aerob.* **2018**, *91*.

18. Costantino, U.; Bugatti, V.; Gorrasi, G.; Montanari, F.; Nocchetti, M.; Tammaro, L.; and Vittoria, V. New polymeric composites based on poly(ε-caprolactone) and layered double hydroxides containing antimicrobial species. *ACS Appl. Mater. Interfaces* **2009**, *1*, 668–677. DOI: 10.1021/am8001988.
19. Bastianini, M.; Costenaro, D.; Bisio, C.; Marchese, L.; Costantino, U.; Vivani, R.; Nocchetti. M.; On the intercalation of the iodine-iodide couple on layered double hydroxides with different particle sizes. *Inorg. Chem.* **2012**, *51*, https://doi.org/10.1021/ic202520v.
20. Bovio, B.; Locchi, S.; Crystal structure of the orthorhombic basic copper nitrate, $Cu_2(OH)_3NO_3$. *Journal of Crystallographic and Spectroscopic Research*, **1982**, *12*, 6. https://doi.org/10.1007/BF01160904.
21. Ruiz, C. V.; Rodríguez-Castellón, E.; Giraldo, O.; Hybrid materials based on a layered zinc hydroxide solid and gallic acid: Structural characterization and evaluation of the controlled release behavior as a function of the gallic acid content. *Appl. Clay Sci.* **2019**, *181*, 105228. https://doi.org/10.1016/j.clay.2019.105228.
22. Nabipour, H.; Sadr, M. H.; Thomas, N. Synthesis, controlled release and antibacterial studies of nalidixic acid-zinc hydroxide nitrate nanocomposites. *New J. Chem.* **2016**, *40*, 238–244. https://doi.org/10.1039/C5NJ01737H.
23. Adam, N.; Mohd Ghazali, S. A. I. S.; Dzulkifli, N. N.; Hak, C. R. C.; Sarijo. S. H. Intercalations and characterization of zinc/aluminium layered double hydroxide-cinnamic acid. *Bull. Chem. React. Eng. Catal.* **2019**, *14*, 165–172. DOI:10.9767/bcrec.14.1.3328.165-172.
24. Pérez, M.R.; Pavlovic, I.; Barriga, C.; Cornejo, J.; Hermosín, M.C.; Ulibarri, M.A.; Uptake of Cu^{2+}, Cd^{2+} and Pb^{2+} on Zn-Al layered double hydroxide intercalated with edta. *Appl. Clay Sci.* **2006**, *32*, 245–251. https://doi.org/10.1016/j.clay.2006.01.008.
25. Palacio, L. A.; Velásquez, J.; Echavarría, A.; Faro, A.; Ribeiro, F. R.; Ribeiro, M. F. Total oxidation of toluene over calcined trimetallic hydrotalcites type catalysts. *J. Hazard. Mater.* **2010**, *177*, 407–413. https://doi.org/10.1016/j.jhazmat.2009.12.048.
26. Mohsin, S.M.N.; Hussein, M.Z.; Sarijo, S.H.; Fakurazi, S.; Arulselven, P.; Yun Hin, T.-Y. Synthesis of (cinnamate-zinc layered hydroxide) intercalation compound for sunscreen application. *Chem. Cent. J.* **2013**, *7*, 1–12. https://doi.org/10.1186/1752-153X-7-26.
27. Arizaga, G. G. C.; Satyanarayana, K. G.; F. Wypych. Layered hydroxide salts: Synthesis, properties and potential applications. *Solid State Ionics* **2007**, *178*, 1143–1162. https://doi.org/10.1016/j.ssi.2007.04.016.
28. Silion, M.; Hritcu, D.; Popa, M. I. Intercalation of salicylic acid into ZnAl layered double hydroxides by ionic-exchange method. *Optoelectron. Adv. Mater. Rapid Commun.* **2009**, *3*, 817–820.
29. Shamraiz, U.; Badshah, A.; Hussain, R. A.; Nadeem, M. A.; Saba, S. Surfactant-Free Fabrication of Copper Sulfides (CuS, Cu2S) via Hydrothermal Method. *J. Clust. Sci.* **2013**, *24*, 1181–1191. https://doi.org/10.1016/j.jscs.2015.07.005.
30. Cheng, H. M.; Gao, X.W.; Kang Zhang, K.; Xin-Rui Wang, X.-R.; Zhou, W.; Li, S.-H.; Cao, X.-L.; Yan, D.-P. A novel antimicrobial composite: ZnAl-hydrotalcite with: P -hydroxybenzoic acid intercalation and its possible application as a food packaging material. *New J. Chem.* **2019**, *43*, 19408–19414. https://doi.org/10.1039/C9NJ03943K.
31. Effah, C. Y.; Sun, T.; Liu, S.; Wu, Y. Klebsiella pneumoniae: An increasing threat to public health. *Ann. Clin. Microbiol. Antimicrob.* **2020**, *19*, 1–9. https://doi.org/10.1186/s12941-019-0343-8.
32. Congradyova, A.; Jomová, K.; Kucková, L.; Kozísek, J.; Moncol, J.; Valko, M. Antimicrobial activity of copper (II) complexes. *The Journal of Microbiology, Biotechnology and Food Sciences*, **2014**, *3*, 67.